

Article

Boundary Layer Flow through Darcy–Brinkman Porous Medium in the Presence of Slip Effects and Porous Dissipation

Muhammad Salman Kausar ¹, Abid Hussanan ^{2,3,*}, Mustafa Mamat ¹ and Babar Ahmad ⁴

¹ Faculty of Informatics and Computing, University Sultan Zainal Abidin (Kampus Gong Badak), Kuala Terengganu, Terengganu 21300, Malaysia; salmanrao603@gmail.com (M.S.K.); must@unisza.edu.my (M.M.)

² Division of Computational Mathematics and Engineering, Institute for Computational Science, Ton Duc Thang University, Ho Chi Minh City 700000, Vietnam

³ Faculty of Mathematics and Statistics, Ton Duc Thang University, Ho Chi Minh City 70000, Vietnam

⁴ Department of Mathematics, COMSATS University Islamabad (CUI) Park Road, Tarlai Kalan, Islamabad 455000, Pakistan; babar.sms@gmail.com

* Correspondence: abidhussanan@tdtu.edu.vn

Received: 20 March 2019; Accepted: 6 May 2019; Published: 11 May 2019



Abstract: This paper aims to examine the Darcy–Brinkman flow over a stretching sheet in the presence of frictional heating and porous dissipation. The governing equations are modeled and simplified under boundary layer approximations, which are then transformed into system of self-similar equations using appropriate transformations. The resulting system of nonlinear equations was solved numerically under velocity and thermal slip conditions, by fourth-order Runge–Kutta method and built-in routine `bvp4c` in Matlab. Under special conditions, the obtained results were compared with the results available in the literature. An excellent agreement was observed. The variation of parameters was studied for different flow quantities of interest and results are presented in the form of tables and graphs.

Keywords: Darcy–Brinkman porous medium; viscous dissipation; slip conditions; porous dissipation; permeable sheet

1. Introduction

The porous medium is a continuous solid phase having void spaces/pores in it. The fraction of the void space to the total volume is named as porosity. There are plenty of porous media available naturally and many of them are artificial. Some examples of porous medium are rocks such as limestone, sand stone, beach sand, pumice and dolomite, lathes packed with pebbles, cloth sponge, rye bread, foamed plastics, endothelial surface layer, catalyst pellets, gall bladder with stones, human lung, and drug permeation through human skin. Industrial and engineering applications of flows through porous medium have attracted the attention of researchers. Purification and filtration processes, seepage of water in river beds, migration of pollutants into the soil and aquifers, drying of porous materials in textile industries, the movement of moisture through and under engineering structures, the saturation of porous materials by chemicals, and heat and mass transport in packed bed reactor columns stand among many other applications. “Flow is linearly dependent on the pressure gradient and the gravitational force” is known as Darcy Law. This law is generally accepted as the macroscopic equation of motion for the Newtonian fluids in porous media at small Reynolds numbers and when the medium is close-packed (lower permeability). However, when the pore distribution in the medium is sparse and the pores are large, the porous medium will have large voids, giving rise to viscous shear in addition to Darcy’s resistance. In that case, the usual viscous resistance term (Brinkman term)

should be considered, along with the Darcy resistance term. This model is known as Darcy–Brinkman model [1–7].

In a stretching flow, an elastic flat sheet that is stretched in its own plane with a velocity changing with the distance from a fixed point. The sheeting material is being produced in numerous manufacturing, industrial and engineering processes. In the manufacture of the polymer sheets, the melt material, when pushed through an extrusion die, cools and solidifies at a distance from the die before reaching the cooling phase. Applications of the boundary layer flow generated by stretching sheet can also be witnessed in procedures such as spinning of fibers, glass blowing, hot rolling, continuous casting, and in thin film flow and many others [8–14]. Boundary layer flow over a stretching sheet in the presence of Darcy porous medium are investigated by several researchers [15–20]. Darcy–Brinkman flow over a stretching sheet was performed by Waqar and Pop [21] and Khan et al. [22]. When fluid is forced to move due to the stretching of sheet, the fluid gains some velocity as well as kinetic energy and this kinetic energy is converted into the heat energy. In the presence of porous medium, viscous dissipation term in energy equation is modified and this phenomenon is called porous dissipation. In [21,22], the authors neglected the viscous dissipation effects. Moreover, even in the case of Darcy flow, the authors neglected the porous dissipation terms in the modeling. From the literature survey and to best of our knowledge, no one has investigated the Darcy–Brinkman flow over a stretching sheet in the presence of frictional heating and porous dissipation.

The phenomenon of slip condition has many industrial and practical applications, especially in microchannels or nanochannels. To study heat transfer flows more accurately, slip conditions are required, which strongly influence fluid motion at the fluid–solid interface. Zhang et al. [23] investigated the heat transfer performance in microchannel under the slip flow regime and constant heat flux boundary condition by considering into account the effects of velocity slip and temperature jump. Hooman and Ejlali [24] showed that the combined effects of temperature jump and velocity slip on forced convection in both parallel plate and circular microchannels for fully developed gas–liquid slip flows. Hussanan et al. [25] studied the Newtonian heating problem with additional effects of velocity slip and free convection on heat transfer flow over a vertical plate. Liu and Guo [26] used second-order slip condition while studying analytical solution of fractional Maxwell flow under magnetic field. Jing et al. [27] investigated the hydraulic resistance and heat transfer rate in elliptical microchannel with the velocity slip for different length ratios. Andersson [28] obtained the analytical solution for the slip flow over a stretching sheet. Turkyilmazoglu [29] performed the heat and mass transfer analysis of MHD flow over a stretching sheet in presence of velocity and thermal slip effects. Yazdi et al. [30] studied the effects of viscous dissipation on MHD flow over a porous stretching sheet in the presence of slip and convective boundary conditions. Hsiao [31] examined the MHD stagnation point flow of nanofluid towards a stretching sheet with slip boundary conditions.

The aim of this paper is to investigate the Darcy–Brinkman flow over a permeable stretching sheet in the presence of viscous and porous dissipation under the velocity and thermal slip conditions. Governing equations are modeled and then transformed into self-similar forms using the suitable similarity transformations. Note that, in the presence of viscous dissipation, similar solutions are very rare. Resulting self-similar equations were solved numerically using shooting method. Comparative study between shooting method and built in routine `bvp4c` [32] in Matlab was also made, to check the accuracy of our results. Moreover, in special cases, comparison between the existing available results was performed. The variations of pertinent parameters on the dimensionless velocity, temperature, skin friction coefficient and local Nusselt number are illustrated and discussed.

2. Mathematical Formulation

We consider the flow of over a permeable stretching surface embedded in a porous medium. In Cartesian coordinates, x -axis and y -axis are perpendicular to the sheet, which is being stretched with velocity $U_s = ax$. Let $T_s = T_\infty + cx^2$ be the temperature of sheet and T_∞ be the ambient temperature

and $T_s > T_\infty$. In the presence of viscous dissipation, governing equations under boundary layer assumption are

$$\frac{\partial u}{\partial x} + \frac{\partial v}{\partial y} = 0, \tag{1}$$

$$u \frac{\partial u}{\partial x} + v \frac{\partial u}{\partial y} = \frac{\varepsilon^2 \mu_e}{\rho} \left(\frac{\partial^2 u}{\partial y^2} \right) - \frac{\mu \varepsilon^2}{\rho K^*} u, \tag{2}$$

$$u \frac{\partial T}{\partial x} + v \frac{\partial T}{\partial y} = \frac{\kappa}{\rho C_p} \left(\frac{\partial^2 T}{\partial y^2} \right) + \frac{\varepsilon^2}{\rho C_p} \left[\mu_e \left(\frac{\partial u}{\partial y} \right)^2 + \frac{\mu u^2}{K^*} \right], \tag{3}$$

along with boundary conditions

$$u = \alpha x + \beta_1 \left(\frac{\partial u}{\partial y} \right), v = -V_0, T = T_s + \delta_1 \left(\frac{\partial T}{\partial y} \right) \text{ at } y = 0, \tag{4}$$

$$u \rightarrow 0, T \rightarrow T_\infty \text{ as } y \rightarrow \infty.$$

In above equations, u and v are the components of velocity along x and y directions, respectively. Introducing the similarity transformations

$$\xi = \sqrt{\frac{\alpha}{v}} y, u = \alpha x g'(\xi), v = -\sqrt{\alpha v} g'(\xi), \theta(\xi) = \frac{T - T_\infty}{T_s - T_\infty}. \tag{5}$$

Equations (1)–(3) along with boundary conditions Equation (4) are reduced to the dimensionless forms

$$\gamma g''' - g'^2 + g g'' - P_m g' = 0, \tag{6}$$

$$\frac{1}{Pr} \theta'' + g \theta' - 2g' \theta + Ec(\gamma g'^2 + P_m g'^2) = 0, \tag{7}$$

$$g(0) = S, g'(0) = 1 + \beta g''(0), g'(\infty) = 0, \tag{8}$$

$$\theta(0) = 1 + \delta \theta'(0), \theta(\infty) = 0.$$

Skin friction coefficients S_{fx} and the local Nusselt number N_{Rx} are defined as

$$S_{fx} = \frac{\mu}{\rho U_s^2} \left(\frac{\partial u}{\partial y} \right)_{y=0}, N_{Rx} = -\frac{x}{(T_s - T_\infty)} \left(\frac{\partial T}{\partial y} \right)_{y=0}. \tag{9}$$

In dimensionless form, quantities defined in Equation (9) take the form

$$S_{fx} Re_x^{1/2} = g''(0), N_{Rx} Re_x^{-1/2} = -\theta'(0). \tag{10}$$

In Equations (6)–(10), dimensionless physical parameters are defined as

Dimensionless Physical Parameters	Notations	Definitions
Brinkmann parameter	γ	$\frac{\varepsilon^2 \mu_e}{\mu}$
Porosity parameter	P_m	$\frac{\mu \varepsilon^2}{\rho \alpha K^*}$
Suction/injection parameter	S	$\frac{V_0}{\sqrt{\alpha v}}$
Prandtl number	Pr	$\frac{\mu C_p}{\kappa}$
Eckert number	Ec	$\frac{\alpha^2}{c C_p}$
Velocity slip parameter	β	$\beta_1 \sqrt{\frac{\alpha}{v}}$
Thermal slip parameter	δ	$\delta_1 \sqrt{\frac{\alpha}{v}}$

3. Solution Methodologies

The nonlinear differential Equations (6) and (7) subject to the boundary conditions in Equation (8) were solved numerically using an efficient Runge–Kutta fourth-order method along with shooting technique. The asymptotic boundary conditions given by Equation (8) were replaced by using a value of 15 for the similarity variable ξ_{\max} . The choice of $\xi_{\max} = 15$ and the step size $\Delta\xi = 0.001$, ensured that all numerical solutions approached the asymptotic values correctly. To check the accuracy of computed results, comparison between analytical, exact and shooting method was made for special cases available in the literature. Moreover, for present general case results obtained by shooting method were also compared with the built-in routine `bvp4c` in MATLAB. The obtained results are in excellent agreement, which confirms the accuracy of our results.

4. Results and Discussion

We analyzed the effects of significant physical parameters on dimensionless velocity $g'(\xi)$, dimensionless temperature $\theta(\xi)$, skin friction coefficient $S_{fx} \text{Re}_x^{1/2} = -g''(0)$ and local Nusselt number $N_{Rx} \text{Re}_x^{-1/2} = -\theta'(0)$. Table 1 presents different values of velocity slip parameter β when there is no porous medium and sheet is impermeable. Skin friction coefficient decreases by increasing the velocity slip parameter. In the case of no-slip i.e., when $\beta = 0$, Equation (6) admits exact solution of the form [22]

$$g(\xi) = S + \frac{1}{A}(1 - e^{-A\xi}), \quad A = \frac{S + \sqrt{S^2 + 4\gamma(1 + P_m)}}{2\gamma}. \tag{11}$$

Table 1. Comparison between analytical solution [22] and shooting method for different values of β when $\gamma = 1$ and $P_m = 0.0, S = 0.0$.

Velocity Slip Parameter β	$g'(0)$		$-g''(0)$	
	Andersson [22]	Present	Andersson [22]	Present
0.0	1.0000	1.0000	1.0000	1.0000
0.1	0.9128	0.91278	0.8721	0.87215
0.2	0.8447	0.84471	0.7764	0.77645
0.5	0.7044	0.70436	0.5912	0.59127
1.0	0.5698	0.56974	0.4302	0.43025
2.0	0.4320	0.43183	0.2840	0.28408
5.0	0.2758	0.27530	0.1448	0.14493
10.0	0.1876	0.18670	0.0812	0.08132
20.0	0.1242	0.12285	0.0438	0.04385
50.0	0.0702	0.06801	0.0186	0.01863
100.0	0.0450	0.04225	0.0095	0.00957

Table 2 shows that the numerical solution obtained by shooting method is in good agreement with the exact solution. Moreover, we observed the skin friction coefficient Brinkman viscosity for parameter γ , whereas an oppose behavior is noted with increasing values suction parameter S and porosity parameter P_m . Table 3 shows that the skin friction coefficient is higher for the slip case in comparison with no-slip case. Numerical values of local Nusselt number for different physical parameters are presented in Table 4. Nusselt number increases by increasing Prandtl number Pr and decreases by increasing Eckert number Ec and thermal slip parameter δ .

Table 2. Skin friction coefficient $S_{fx}Re_x^{1/2} = -g''(0)$ for no slip case $\beta = 0$. Comparison between exact and numerical solution.

Physical Parameters			$S_{fx}Re_x^{1/2} = -g''(0)$	
γ	S	P_m	Exact (See Equation (11))	Numerical (Shooting Method)
1.0	1.0	0.5	1.82287	1.82287
2.0	1.0	0.5	1.15138	1.15140
3.0	1.0	0.5	0.89314	0.89324
0.5	0.0	0.3	1.61245	1.61245
0.5	1.0	0.3	2.89736	2.89736
0.5	2.0	0.3	4.56904	4.56905
2.0	0.5	0.0	0.84307	0.84336
2.0	0.5	0.4	0.97094	0.97098
2.0	0.5	0.8	1.08188	1.08188

Table 3. Skin friction coefficient $S_{fx}Re_x^{1/2} = -g''(0)$ for slip case $\beta = 1.0$. Comparison between Shooting method and MATLAB bvp4c.

Physical Parameters			$S_{fx}Re_x^{1/2} = -g''(0)$	
γ	S	P_m	Shooting Method	bvp4c
1.0	1.0	0.5	0.610511	0.610497
2.0	1.0	0.5	0.500008	0.500006
3.0	1.0	0.5	0.439566	0.439507
0.5	0.0	0.3	0.550438	0.550437
0.5	1.0	0.3	0.712228	0.712227
0.5	2.0	0.3	0.808872	0.808872
2.0	0.5	0.0	0.406493	0.406209
2.0	0.5	0.4	0.452006	0.451987
2.0	0.5	0.8	0.485908	0.485905

Table 4. Local Nusselt number $N_{Rx}Re_x^{-1/2} = -\theta'(0)$ when $\beta = 1.0$ and $S = 0.5$ Comparison between Shooting method and MATLAB bvp4c.

Physical Parameters					$N_{Rx}Re_x^{-1/2} = -\theta'(0)$	
Pr	Ec	δ	P_m	γ	Shooting Method	bvp4c
0.7	0.5	1.0	0.4	2.0	0.456141	0.456203
1.2	0.5	1.0	0.4	2.0	0.538161	0.538197
6.8	0.5	1.0	0.4	2.0	0.738928	0.738983
3.0	0.0	1.0	0.4	2.0	0.738078	0.738124
3.0	0.6	1.0	0.4	2.0	0.642319	0.642382
3.0	1.2	1.0	0.4	2.0	0.546560	0.546591
3.0	1.0	0.0	0.4	2.0	2.208602	2.208638
3.0	1.0	0.6	0.4	2.0	0.820808	0.820821
3.0	1.0	1.2	0.4	2.0	0.504071	0.504105
3.0	1.0	1.0	0.0	2.0	0.640207	0.640288
3.0	1.0	1.0	0.5	2.0	0.566207	0.566224
3.0	1.0	1.0	1.0	2.0	0.517044	0.517133
3.0	1.0	1.0	0.4	1.0	0.619665	0.619690
3.0	1.0	1.0	0.4	2.0	0.578480	0.578501
3.0	1.0	1.0	0.4	3.0	0.546450	0.546487

Figure 1 is plotted to see effect of Brinkman viscosity ratio parameter γ on velocity profile. It was observed that velocity increases on increasing the values of Brinkman viscosity ratio number. This also makes the sense because the Brinkman viscosity ratio number appears with the velocity gradient term in the momentum equation, consequently large values of Brinkman viscosity parameter increases the velocity. Figure 2 portrays the effects of porosity parameter P_m on the velocity profile. It was observed that velocity and momentum boundary layer decreases by increasing porosity parameter. In Figures 3 and 4, we can see that, by increasing the suction parameter S and slip parameter β , the velocity of fluid decreases and momentum boundary layer becomes thinner. Figure 5 displays the impact of Brinkman viscosity number on the temperature profile $\theta(\xi)$. Thermal boundary layer is an increasing function of γ . Increase in the suction velocity S and porosity parameter P_m decreases the fluid temperature with in the boundary layer (see Figures 6 and 7). Figure 8 exhibits the influence of Prandtl number on the temperature field $\theta(\xi)$. Temperature inside the boundary layer decreases with increasing Prandtl number Pr . This is true because, by increasing Prandtl number (decreasing thermal conductivity) of fluid, the heat transfer rate from the stretching sheet decreases and therefore thermal boundary layer decreases. Figure 9 depicts the influence of Eckert number Ec on temperature profile. As predictable, it is noticed that the thermal boundary layer increases with increasing values of Ec as Eckert number increases fluid friction between the adjacent layers increases, which results in conversion of the kinetic energy into heat energy. Figure 10 illustrates that temperature and thermal boundary layer reduces by increasing thermal slip parameter δ .

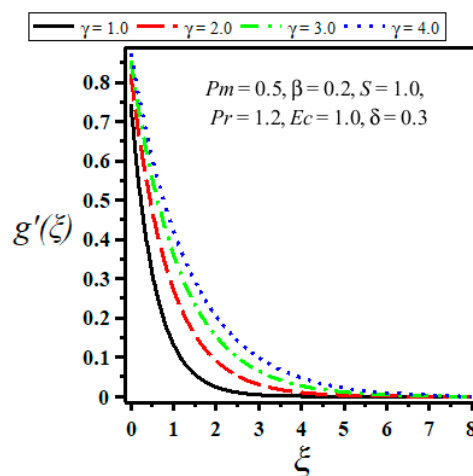


Figure 1. Variation of velocity with viscosity ratio parameter γ .

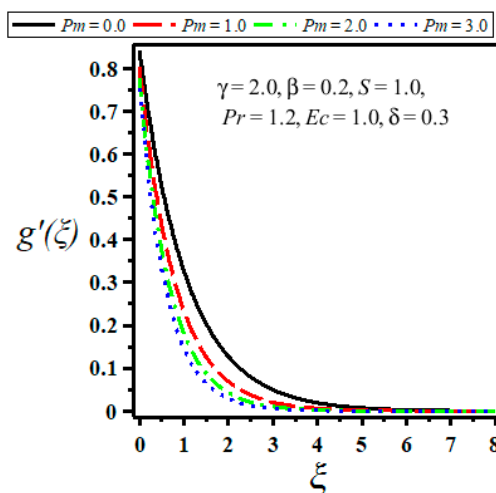


Figure 2. Variation of velocity with porosity parameter P_m .

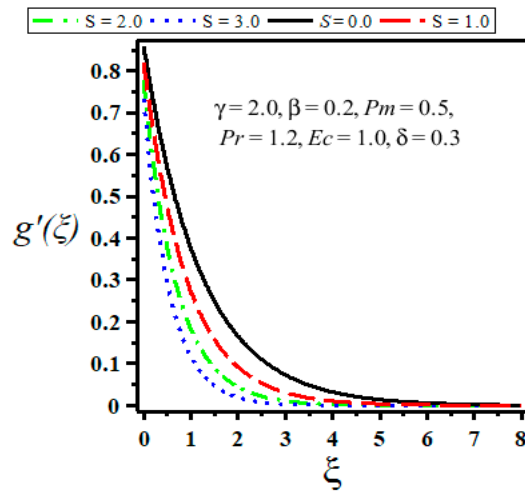


Figure 3. Variation of velocity with suction parameter S .

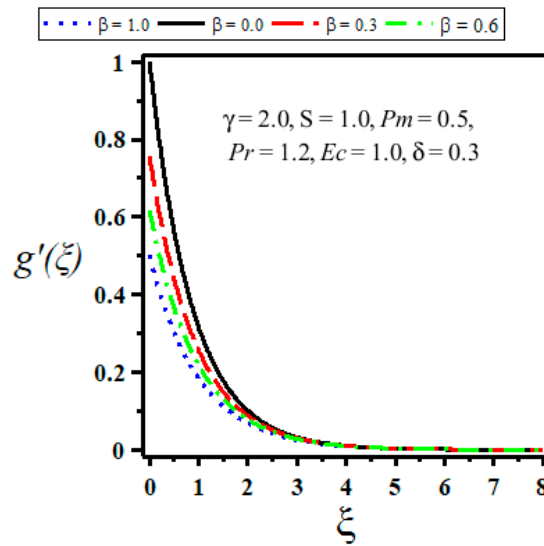


Figure 4. Variation of velocity with velocity slip parameter β .

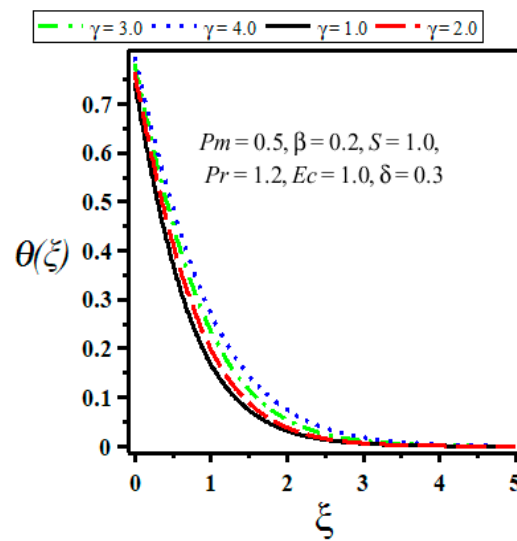


Figure 5. Variation of temperature with Brinkman parameter γ .

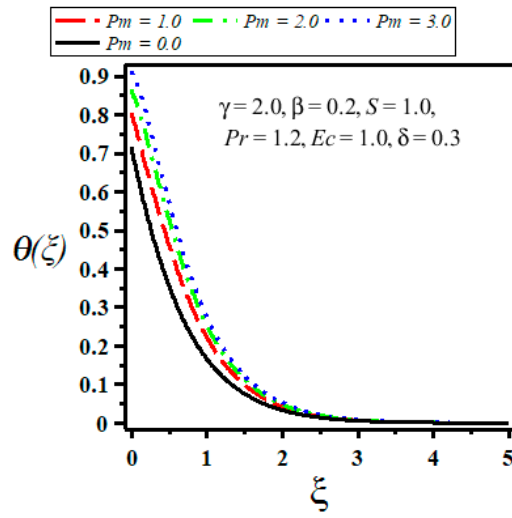


Figure 6. Variation of temperature with porosity parameter P_m .

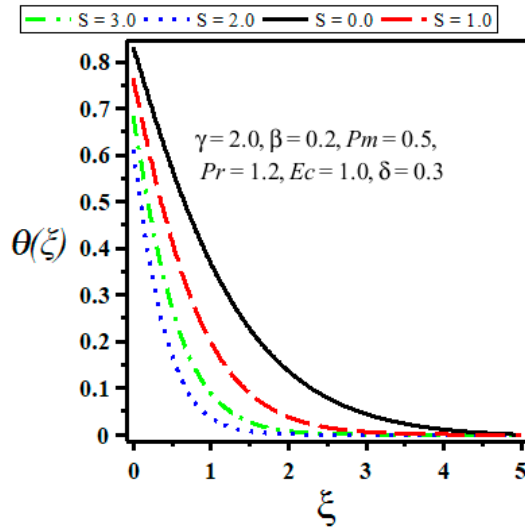


Figure 7. Variation of temperature with suction parameter S .

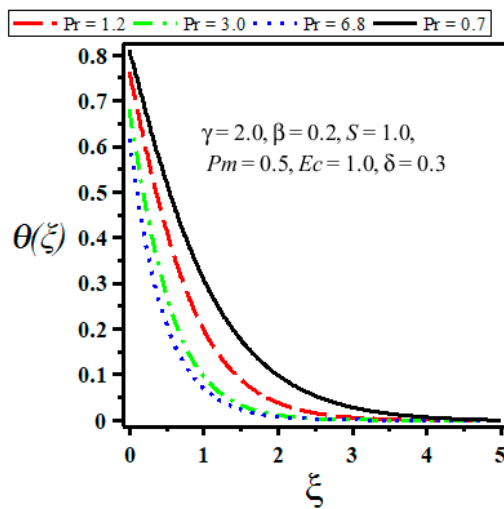


Figure 8. Variation of temperature with Prandtl number Pr .

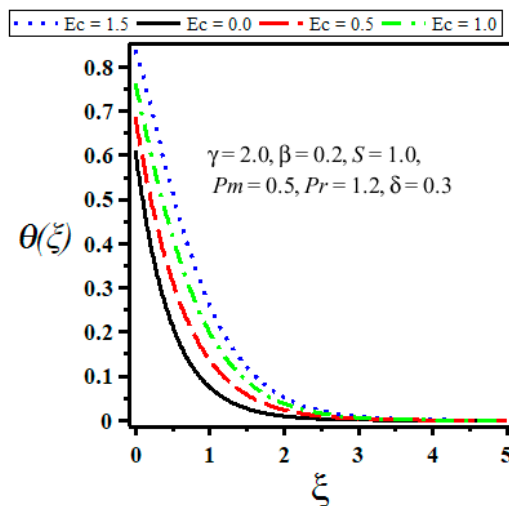


Figure 9. Variation of temperature with Eckert number Ec .

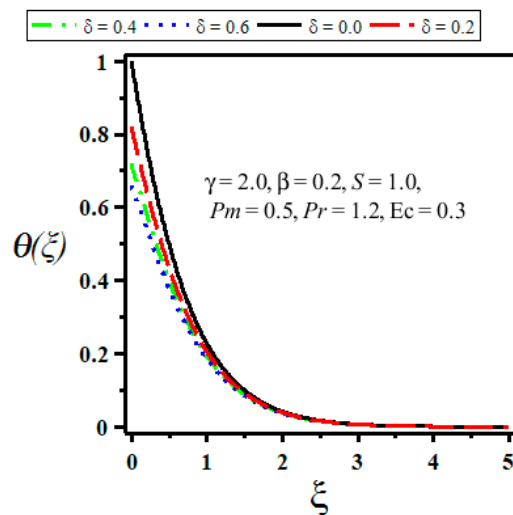


Figure 10. Variation of temperature with thermal slip parameter δ .

5. Conclusions

The present work gives the numerical solutions for Darcy–Brinkman flow over a stretching sheet in the presence of porous dissipation and frictional heating. From the numerical results obtained, some important conclusions are summarized:

- (i) Both velocity and temperature decrease with the increase of suction parameter.
- (ii) The slip parameter has high impact on skin friction coefficient as compared with no-slip condition.
- (iii) Heat transfer rate is reduced due to increase in Eckert number and thermal slip parameter.

Author Contributions: M.S.K. and A.H. formulated the problem. M.S.K. and B.A. solved the problem. M.S.K., A.H., M.M. and B.A. computed and analyzed the results. All the authors equally contributed in writing and proof reading of the paper.

Funding: The APC was funded by Ton Duc Thang University, Ho Chi Minh City, Vietnam.

Conflicts of Interest: The authors declare no conflict of interest.

References

1. Patil, P.R.; Vaidyanathan, G. Effect of variable viscosity on thermohaline convection in a porous medium. *J. Hydrol.* **1982**, *57*, 147–161. [[CrossRef](#)]
2. Ingham, D.B.; Pop, I. *Transport Phenomena in Porous Media*; Elsevier: Amsterdam, The Netherlands, 1998.
3. Vafai, K. *Handbook of Porous Media*; CRC Press: Boca Raton, FL, USA, 2005.
4. Makinde, O.D.; Mhone, P.Y. Heat transfer to MHD oscillatory flow in a channel filled with porous medium. *Rom. J. Phys.* **2005**, *50*, 931–938.
5. Yu, L.H.; Wang, C.Y. Darcy-Brinkman flow through a bumpy channel. *Transp. Porous Media* **2013**, *97*, 281–294. [[CrossRef](#)]
6. Wang, C.Y. Darcy-Brinkman flow over a grooved surface. *Transp. Porous Media* **2010**, *84*, 219–227. [[CrossRef](#)]
7. Liu, H.; Patil, P.R.; Narusawa, U. On Darcy-Brinkman equation: Viscous flow between two parallel plates packed with regular square arrays of cylinders. *Entropy* **2007**, *9*, 118–131. [[CrossRef](#)]
8. Crane, L.J. Flow past a stretching plate. *Z. Angew. Math. Phys. Zamp* **1970**, *4*, 645–647. [[CrossRef](#)]
9. Ishak, A.; Nazar, R.; Pop, I. Hydromagnetic flow and heat transfer adjacent to a stretching vertical sheet. *Heat Mass Transf.* **2008**, *44*, 921–927. [[CrossRef](#)]
10. Chamkha, A.J. Hydromagnetic three-dimensional free convection on a vertical stretching surface with heat generation or absorption. *Int. J. Heat Fluid Flow* **1999**, *20*, 84–92. [[CrossRef](#)]
11. Salleh, M.Z.; Nazar, R.; Pop, I. Boundary layer flow and heat transfer over a stretching sheet with Newtonian heating. *J. Taiwan Inst. Chem. Eng.* **2010**, *41*, 651–655. [[CrossRef](#)]
12. Hsiao, K.L. Micropolar nanofluid flow with MHD and viscous dissipation effects towards a stretching sheet with multimedia feature. *Int. J. Heat Mass Transf.* **2017**, *112*, 983–990. [[CrossRef](#)]
13. Hussanan, A.; Salleh, M.Z.; Khan, I. Microstructure and inertial characteristics of a magnetite ferrofluid over a stretching/shrinking sheet using effective thermal conductivity model. *J. Mol. Liq.* **2018**, *255*, 64–75. [[CrossRef](#)]
14. Jamaludin, A.; Nazar, R.; Pop, I. Mixed convection stagnation-point flow of a nanofluid past a permeable stretching/shrinking sheet in the presence of thermal radiation and heat source/sink. *Energies* **2019**, *12*, 788. [[CrossRef](#)]
15. Mukhopadhyay, S. Effect of thermal radiation on unsteady mixed convection flow and heat transfer over a porous stretching surface in porous medium. *Int. J. Heat Mass Transf.* **2009**, *52*, 3261–3265. [[CrossRef](#)]
16. Chauhan, D.S.; Agrawal, R. MHD flow through a porous medium adjacent to a stretching sheet: Numerical and an approximate solution. *Eur. Phys. J. Plus* **2011**, *126*, 47. [[CrossRef](#)]
17. Pal, D.; Mondal, H. Influence of chemical reaction and thermal radiation on mixed convection heat and mass transfer over a stretching sheet in Darcian porous medium with Soret and Dufour effects. *Energy Convers. Manag.* **2012**, *62*, 102–108. [[CrossRef](#)]
18. Zheng, L.; Zhang, C.; Zhang, X.; Zhang, J. Flow and radiation heat transfer of a nanofluid over a stretching sheet with velocity slip and temperature jump in porous medium. *J. Frankl. Inst.* **2013**, *350*, 990–1007. [[CrossRef](#)]
19. Hussanan, A.; Salleh, M.Z.; Khan, I.; Tahar, R.M. Heat transfer in magnetohydrodynamic flow of a casson fluid with porous medium and Newtonian heating. *J. Nanofluids* **2017**, *6*, 784–793. [[CrossRef](#)]
20. Yasin, M.H.M.; Ishak, A.; Pop, I. Boundary layer flow and heat transfer past a permeable shrinking surface embedded in a porous medium with a second-order slip: A stability analysis. *Appl. Therm. Eng.* **2017**, *115*, 1407–1411. [[CrossRef](#)]
21. Khan, W.A.; Pop, I. Boundary layer flow past a stretching surface in a porous medium saturated by a nanofluid: Brinkman-Forchheimer model. *PLoS ONE* **2012**, *7*, e47031. [[CrossRef](#)]
22. Khan, Z.H.; Qasim, M.; Haq, R.U.; Al-Mdallal, Q.M. Closed form dual nature solutions of fluid flow and heat transfer over a stretching/shrinking sheet in a porous medium. *Chin. J. Phys.* **2017**, *55*, 1284–1293. [[CrossRef](#)]
23. Zhang, T.; Jia, L.; Yang, L.; Jaluria, Y. Effect of viscous heating on heat transfer performance in microchannel slip flow region. *Int. J. Heat Mass Transf.* **2010**, *53*, 4927–4934. [[CrossRef](#)]
24. Hooman, K.; Ejlali, A. Effects of viscous heating, fluid property variation, velocity slip, and temperature jump on convection through parallel plate and circular microchannels. *Int. Commun. Heat Mass Transf.* **2010**, *37*, 34–38. [[CrossRef](#)]

25. Hussanan, A.; Khan, I.; Salleh, M.Z.; Shafie, S. Slip effects on unsteady free convective heat and mass transfer flow with Newtonian heating. *Therm. Sci.* **2016**, *20*, 1939–1952. [[CrossRef](#)]
26. Liu, Y.; Guo, B. Effects of second-order slip on the flow of a fractional Maxwell MHD fluid. *J. Assoc. Arab Univ. Basic Appl. Sci.* **2017**, *24*, 232–241. [[CrossRef](#)]
27. Jing, D.; Song, S.; Pan, Y.; Wang, X. Size dependences of hydraulic resistance and heat transfer of fluid flow in elliptical microchannel heat sinks with boundary slip. *Int. J. Heat Mass Transf.* **2018**, *119*, 647–653. [[CrossRef](#)]
28. Andersson, H.I. Slip flow past a stretching surface. *Acta Mech.* **2002**, *158*, 121–125. [[CrossRef](#)]
29. Turkyilmazoglu, M. Analytic heat and mass transfer of the mixed hydrodynamic/thermal slip MHD viscous flow over a stretching sheet. *Int. J. Mech. Sci.* **2011**, *53*, 886–896. [[CrossRef](#)]
30. Yazdi, M.H.; Abdullah, S.; Hashim, I.; Sopian, K. Effects of viscous dissipation on the slip MHD flow and heat transfer past a permeable surface with convective boundary conditions. *Energies* **2011**, *4*, 2273–2294. [[CrossRef](#)]
31. Hsiao, K.L. Stagnation electrical MHD nanofluid mixed convection with slip boundary on a stretching sheet. *Appl. Therm. Eng.* **2016**, *98*, 850–861. [[CrossRef](#)]
32. Shampine, L.F.; Kierzenka, J. Solving boundary value problems for ordinary differential equations in MATLAB with `bvp4c`. *Tutor. Notes* **2000**, *2000*, 1–27.



© 2019 by the authors. Licensee MDPI, Basel, Switzerland. This article is an open access article distributed under the terms and conditions of the Creative Commons Attribution (CC BY) license (<http://creativecommons.org/licenses/by/4.0/>).